

## A Novel Computed Tomography-Ultrasound Image Fusion Technique for Guiding the Percutaneous Kidney Access

Xiaobo Shen<sup>1,2,3\*</sup>, Kaiwen Li<sup>1,2,3\*</sup>, Zhenyu Wu<sup>1,2,3</sup>, Cheng Liu<sup>1,2,3</sup>, Hao Yu<sup>1,2,3</sup>, Cong Lai<sup>1,2,3</sup>, Zhuang Tang<sup>1,2,3</sup>, Kuiqing Li<sup>1,2,3</sup>, Kewei Xu<sup>1,2,3</sup>

**Purpose:** To describe the feasibility of computed tomography (CT)-ultrasound image fusion technique on guiding percutaneous kidney access in vitro and vivo.

**Materials and Methods:** we compare CT-ultrasound image fusion technique and ultrasound for percutaneous kidney puncture guidance by using an in vitro pig kidney model. The fusion method, fusion time, ultrasound screening time, and success rate of puncture were compared between the groups. Next, patients with kidney stones in our hospital were randomized in the study of simulated puncture guidance. The general condition of patients, fusion method, fusion time, and ultrasound screening time were compared between the groups.

**Results:** A total of 45 pig models were established, including 23 in the CT-ultrasound group and 22 in the ultrasound group. The ultrasound screening time in the CT-ultrasound group was significantly shorter than that in the ultrasound group ( $P < .001$ ). In addition, the success rate of puncture in the CT-ultrasound group was significantly higher than that in the ultrasound group ( $P = .015$ ). Furthermore, in the simulated PCNL puncture study, baseline data including age, BMI, and S.T.O.N.E score between the two groups showed no statistical difference. The ultrasound screening time of the two groups was  $(2.60 \pm 0.33)$  min and  $(3.37 \pm 0.51)$  min respectively, and the difference was statistically significant ( $P < .001$ ).

**Conclusion:** Our research revealed that the CT-ultrasound image fusion technique was a feasible and safe method to guide PCNL puncture. Compared with traditional ultrasound guidance, the CT-ultrasound image fusion technique can shorten the learning curve of PCNL puncture, improve the success rate of puncture, and shorten the ultrasound screening time.

**Keywords:** kidney stone; percutaneous nephrolithotomy; computed tomography; ultrasound; puncture

### INTRODUCTION

Kidney stone is one of the most common urological diseases around the world. Due to the high stone free rate (SFR), percutaneous nephrolithotomy (PCNL) has been introduced for the treatment of patients with large kidney stones ( $> 20$  mm)<sup>(1)</sup>. The outcomes of PCNL are highly related to the accuracy of percutaneous kidney puncture in the targeted calyx<sup>(2,3)</sup>. Appropriate percutaneous renal access can guarantee the effectiveness and safety of PCNL and reduce the risk of complications<sup>(4)</sup>.

This challenging step can be accomplished by ultrasound and fluoroscopy, both of which have their shortcomings that may increase the risk of complications<sup>(5,6)</sup>. It is well known that computed tomography (CT) scan is the gold-standard modality for the diagnosis of kidney stones and preoperative planning of PCNL due to its high sensitivity and specificity, precise stone sizing, and the feasibility of evaluating non-stone pathologies<sup>(7)</sup>. Therefore, we proposed to integrate the preoperative CT images into intraoperative ultrasound images to im-

prove the accuracy of percutaneous kidney puncture. CT-ultrasound image fusion technique has shown advantages in the treatment of other diseases. Xu et al.<sup>(8)</sup> have reported that 92 patients with malignant liver tumors underwent radiofrequency ablation (RFA) under the guidance of CT-ultrasound fusion image, proving that fusion technique assisted RFA was a safe and effective option. As a result, our research aimed to apply the CT-ultrasound image fusion method to guide percutaneous kidney puncture and expected to increase the efficiency of stone removal and reduce the risk of complications.

Therefore, the research explored the feasibility of CT-ultrasound image fusion method in establishing an appropriate renal channel. First, we utilized an in vitro pig kidney model to study the feasibility of CT-ultrasound fusion in establishing a percutaneous kidney access. Next, we performed the simulated CT-ultrasound image fusion on patients with kidney stones, further exploring the feasibility of CT-ultrasound fusion method in guiding PCNL puncture.

<sup>1</sup>Department of Urology, Sun Yat-sen Memorial Hospital, Sun Yat-sen University, Guangzhou, Guangdong, P. R. China.

<sup>2</sup>Guangdong Provincial Key Laboratory of Malignant Tumor Epigenetics and Gene Regulation, Sun Yat-sen Memorial Hospital, Sun Yat-sen University, Guangzhou, Guangdong, P. R. China.

<sup>3</sup>Guangdong Provincial Clinical Research Center for Urological Diseases.

\*Equal contribution

\*Correspondence: ? Department of Urology, Sun Yat-sen Memorial Hospital, Sun Yat-sen University, Guangzhou, Guangdong, P. R. China.

Received October 2022 & Accepted February 2023

**Table 1.** Characteristics of CT-ultrasound and ultrasound group in pig kidney model

Variables <sup>a</sup>	CT-ultrasound group	Ultrasound group	P-value
Sample size, n	22	23	-
Chicken weight, kg; mean ± SD	3.44 ± 0.23	3.52 ± 0.28	.326
Length of pig kidney, cm; mean ± SD	12.44 ± 0.75	12.45 ± 0.94	.951
Width of pig kidney, cm; mean ± SD	4.75 ± 0.38	4.72 ± 0.43	.846
Number of artificial stones, n	2 (2~3)	2(2~3)	.661
Image fusion method, n	-	-	-
Long axis of kidney and kidney stones	-	23	-
Fusion time, min; mean ± SD	4.02 ± 0.54	-	-
Ultrasound screening time, min; mean ± SD	2.52 ± 0.31	3.38 ± 0.50	< .001
Puncture depth, cm; mean ± SD	5.99 ± 0.71	5.76 ± 0.80	.306
Puncture success rate, n; (%)	19(86.4)	11(47.8)	.015

**Abbreviations:** CT, computed tomography

<sup>a</sup>Continuous variables were compared by independent samples *t*-test

## MATERIALS AND METHODS

### *In vitro pig kidney model*

For the *in vitro* study, a well-established model was applied to modulate the percutaneous kidney puncture<sup>(9)</sup>. The porcine kidneys and chicken carcasses were bought from commercial slaughterhouse. We incised the renal pelvis and inserted 2-3 artificial stones (10-20 mm) into the calyces through the incision. The prepared pig kidney was placed inside the eviscerated chicken carcass, and filled the remaining space with agar. After the agar was fixed, all the openings of the chicken carcass were closed with sutures to simulate a confined space (Figure 1). A total of 45 models were established, including 23 in the CT-ultrasound group and 22 in the ultrasound group.

### *Patient selection*

Patients in our hospital from December 2019 to February 2021 were enrolled in the simulated PCNL puncture study, who were randomly divided into CT-ultrasound group and ultrasound group with the help of SAS software. The inclusion criteria were as follows: (1) renal pelvis and upper or middle calyx stones with a diameter of more than 2 cm; lower renal calyx stones with a diameter of more than 1.5 cm; (2) available urinary CT data; (3) patients were voluntarily participated and signed an informed consent. Exclusion criteria were patients with anatomical structure or location of the kidney, such as horseshoe kidney, polycystic kidney, pelvic heterotopic kidney, etc. Informed consent was taken from all eligible patients. This study was approved by the ethics committee of our hospital, whose ethical number was 2020-KY-021, and has been registered in ClinicalTrials.gov (NCT04645472).

### *Equipment and Techniques*

The urinary CT image data were acquired using the Optima 64-multidetector helical CT scanner (GE Healthcare, Waukesha, WI) 1 month or less before the procedure. All images were obtained with 1.25-mm-thick sections and a 1:1 pitch. The CT-ultrasound image fusion was achieved by the Real-time Virtual Sonography (RVS) method using the ARIETTA 70 ultrasound system (Hitachi Aloka Medical Ltd., Tokyo, Japan, (Figure 2). Prior to the CT-ultrasound image fusion, the DICOM volume data of the kidney were loaded onto the ARIETTA 70 ultrasound system, and the magnetic generator was placed next to the working area. The image fusion of ultrasound and CT was executed sequentially by the RVS method by the professional ultrasound technician. In this step, we need to find out an image

fusion region, which can be well visualized on both CT and ultrasound images, we can adjust the corresponding ultrasound image to match the CT plane through the image fusion region.

### *Establishment of percutaneous kidney access in the pig kidney model*

Pig kidney models were randomly divided into the CT-ultrasound group and ultrasound group. We found that CT and ultrasound image can be fused using the long axis of the kidney and stones in the CT-ultrasound group. After the fusion was completed, the ultrasound probe was used to investigate the sonographic characteristics of hydronephrosis, stones, renal cortex, and medulla of the porcine kidney so to determine the targeted calyx. We punctured the targeted calyx from the fornix of the calyx. It was defined as a successful puncture when the puncture needle passed through the fornix to reach the targeted calyx after the kidney was opened (Figure 3). In the ultrasound group, we used traditional ultrasound for screening and puncture. Finally, the puncture results of the CT-ultrasound group and the ultrasound group were compared.

### *Simulated PCNL puncture in patients*

We randomly divided the selected patients into the CT-ultrasound group and ultrasound group. In the CT-ultrasound group, according to the previous study<sup>(8)</sup> and our existing experience, we using the long axis of the kidney and stones as the image fusion region to match the corresponding ultrasound image and the CT plane, since right kidney is adjacent to liver, the liver portal system can also be the image fusion region in right kidney (Figure 4). The targeted renal calyx and simulated puncture site were determined based on the stone location, hydronephrosis and adjacent organs. Notably in the CT-ultrasound group, we first determined the learning curve of the CT-ultrasound fusion technique. After the fusion time and ultrasound screening time reached the plateau, the CT-ultrasound group and ultrasound group were compared.

### *Statistical analysis*

SPSS 20.0 software was utilized for statistical analysis. The data were expressed as the mean ± standard deviation or median ± range, and qualitative variables were expressed as the rate. The independent *t* test was applied to compare quantitative variables between the two groups. Normality and homogeneity of variance were also checked. The qualitative variables were compared using the Chi-square test, when no expected cell count less than 1 and at most 20% of expected cell counts less

**Table 2.** Demographic characteristics of CT-ultrasound and ultrasound group in simulated puncture guidance

Variables <sup>a</sup>	CT-ultrasound group	Ultrasound group	P-value
Sample size, n	52	53	-
Gender, n; (%)		.359	
Male	34 (65.4)	29 (54.7)	
Female	18 (34.6)	24 (45.3)	
Laterality, n; (%)		1	
Right	28 (53.8)	29 (54.7)	
Left	24 (46.2)	24 (45.3)	
Age, year; mean ± SD (range)	54.15 ± 11.65 (24-81)	52.74 ± 11.49 (43-82)	.532
BMI, kg/m <sup>2</sup> ; mean ± SD (range)	23.69 ± 3.98 (16.89-41.32)	23.37 ± 3.33 (18.07-32.47)	.653
Previous ipsilateral surgery history, n; (%)	10 (19.2%)	10 (18.9%)	1
Stone size, mm; median (IQR)	19.2 (22)	21.1 (17.6)	.354
Tract length, mm; mean ± SD	82.79 ± 15.24	80.15 ± 13.73	.354
Obstruction or hydronephrosis, n; (%)			.828
None or mild hydronephrosis	37 (71.2)	37 (69.8)	
Moderate hydronephrosis	10 (19.2)	9 (17.0)	
Heavy hydronephrosis 5 (9.6)	7 (13.2)		
Number of involved calyces, n	2.40 ± 1.16	2.33 ± 0.91	.385
Stone density, HU; mean ± SD	1122.71 ± 371.29	1022.32 ± 323.91	.143
S.T.O.N.E score (range)	7 (5-10)	7 (5-10)	.356

**Abbreviations:** BMI, Body Mass Index; IQR, Interquartile Range

<sup>a</sup> Continuous variables were compared by independent samples t-test

than 5. A value of  $p < .05$  was considered statistically significant.

## RESULTS

The detailed results of the in vitro study were shown in **Table 1**. A total of 45 models were established, in-

cluding 23 in the CT-ultrasound group and 22 in the ultrasound group. There were no statistically significant differences in chicken weight, the length and width of kidney between the two groups. The ultrasound screening time in the CT-ultrasound group was significantly shorter than that in the ultrasound group ( $P < .001$ ). In

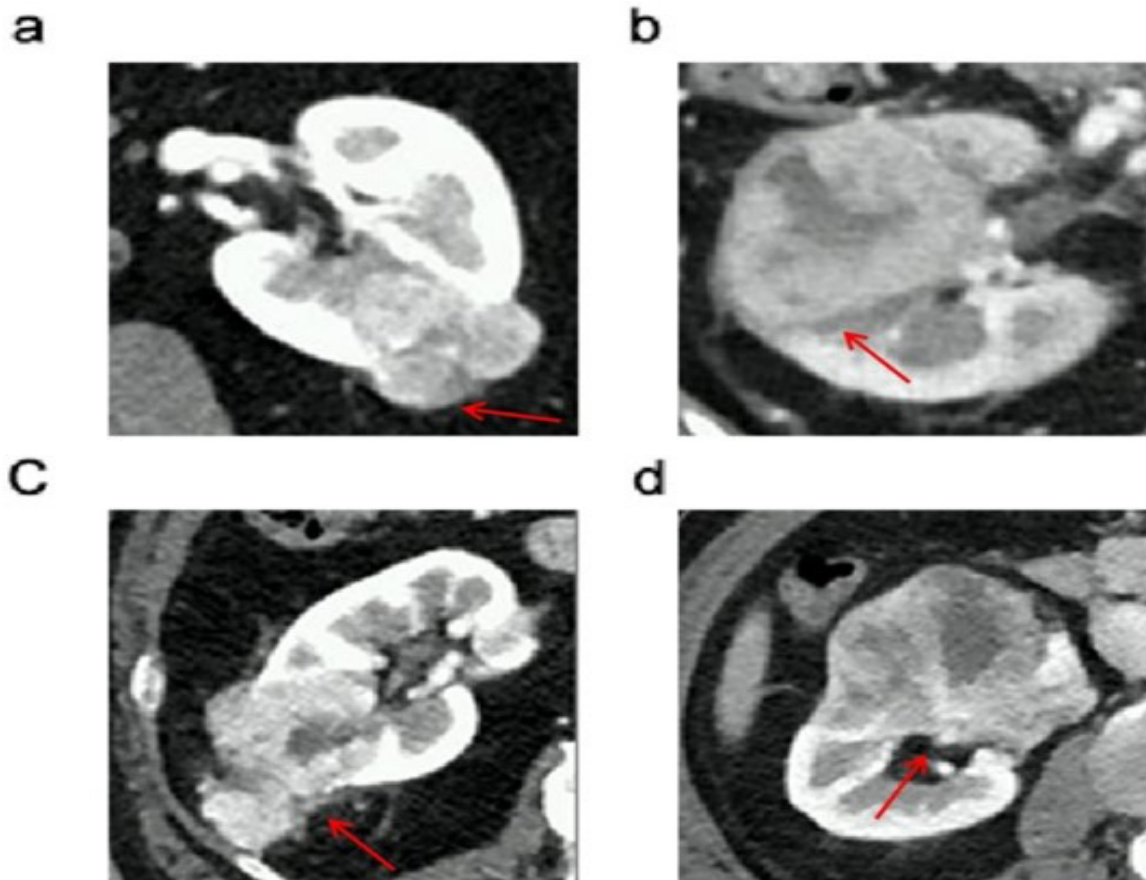


**Figure 1.** Irregular tumor edge of renal cell carcinoma in contrast-enhanced CT (A) A mass with smooth margin and prominent nodules from part of it; (B) A mass with blurred margin; (C) A mass with completely irregular and non-elliptical shape; (D) Renal sinus compression in contrast-enhanced CT

**Table 3.** Outcomes of CT-ultrasound and ultrasound group in simulated puncture guidance

Variables <sup>a</sup>	CT-ultrasound group	Ultrasound group	P-value
Sample size, n	52	53	-
Image fusion region, n; (%)	-	-	-
Portal vein	18 (34.6)	-	-
Long kidney axis and stones (right kidney)	10 (19.2)	-	-
Long kidney axis and stones (left kidney)	24 (46.2)	-	-
Fusion time, min; mean $\pm$ SD	4.27 $\pm$ 0.56	-	-
Ultrasound screening time, min; mean $\pm$ SD (range)	2.60 $\pm$ 0.33 (2.0-3.2)	3.37 $\pm$ 0.51 (2.2-4.3)	< .001
Simulated puncture site, n; (%)	-	-	.331
Above the 12th rib	15 (28.8)	10 (18.9)	
Below the 12th rib	37 (71.2)	43 (81.1)	
Target calyx, n; (%)	-	-	.818
Upper calyx	3 (5.8)	2 (3.8)	
Lower calyx	2 (3.8)	3 (5.6)	
Middle calyx	47 (90.4)	48 (90.6)	

<sup>a</sup>Continuous variables were compared by independent samples *t*-test

addition, the success rate of puncture in the CT-ultrasound group was significantly higher than that in the ultrasound group ( $P = .015$ ).

A total of 150 patients were included in the simulated PCNL puncture study, of which 97 cases in the CT ultrasound group and 53 cases in the ultrasound group. We first determined the learning curve of the CT-ultrasound image fusion method, indicating that the screening time of the CT-ultrasound group reached a plateau after 31-45 cases. Therefore, the last 52 patients in the CT-ultrasound group and 53 patients in the ultrasound group were included in the comparison. There was no statistical difference in baseline data between the two groups (Table 2). The fusion time in the CT-ultrasound group was (4.27  $\pm$  0.56) min. Eighteen cases of the right kidney were fused with the portal venous system; 10 cases were fused with the long axis of the kidney and stones; and all cases of the left kidney were fused with the long axis of the kidney and stones. The ultrasound screening time of the two groups was (2.60  $\pm$  0.33) min and (3.37  $\pm$  0.51) min, respectively, and the difference was statistically significant ( $P < .001$ , Table 3).

## DISCUSSION

In 1976, Fernstrom et al.<sup>(10)</sup> first reported the experience of removing kidney stones through percutaneous nephrostomy, which had been widely used since the early 1980s. Currently, PCNL is recommended for the treatment of upper urinary tract stones with a diameter > 2cm and complex kidney stones owing to its high efficiency and minimal invasiveness. Establishing percutaneous renal access is the most critical step in PCNL. Incorrect puncture can easily damage the blood vessels, thereby increasing the risk of complications such as bleeding and renal function damage<sup>(11)</sup>. Therefore, how to accurately puncture the targeted calyx has become the biggest problem for PCNL.

Rassweiler et al.<sup>(12)</sup> has reported an iPad-assisted technique with a three-dimensional reconstruction and marker tracking method for kidney puncture. Before the surgery, patients underwent a preoperative CT in the prone position with 5 colored metal markers around the puncture site. The CT images were segmented and analyzed to establish a three-dimensional construction and adjacent organ anatomy on an iPad. During

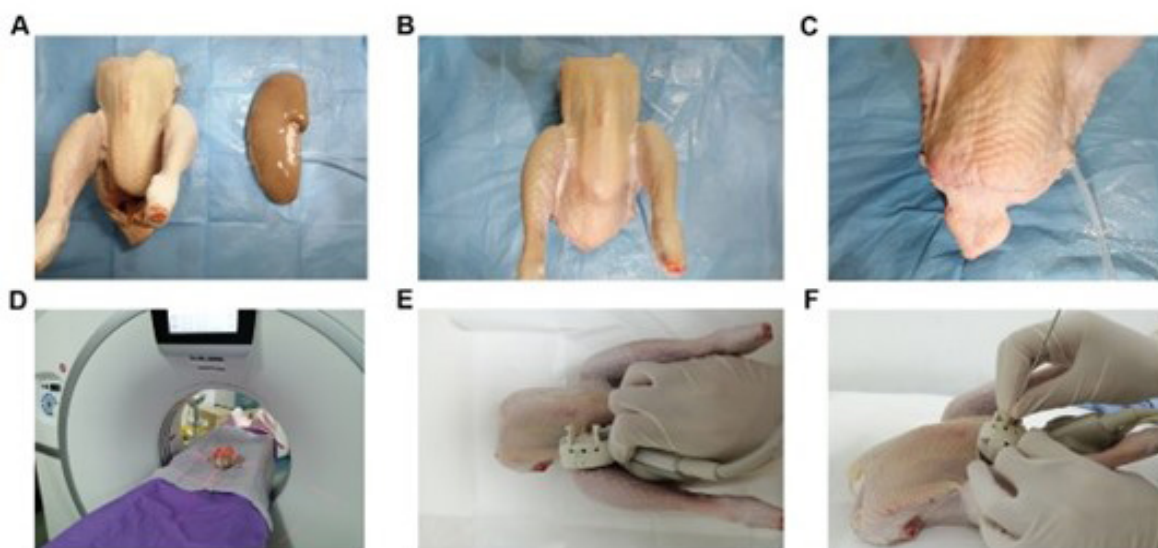


**Figure 1.** Establishment of percutaneous kidney access with the in vitro pig kidney model. (A) Preparation of in vitro pig kidney model. (B) Establishment of in vitro pig kidney model. (C) Suture of the openings. (D) CT scan of the model. (E) Ultrasound screening before puncture. (F) Percutaneous kidney puncture with the model.

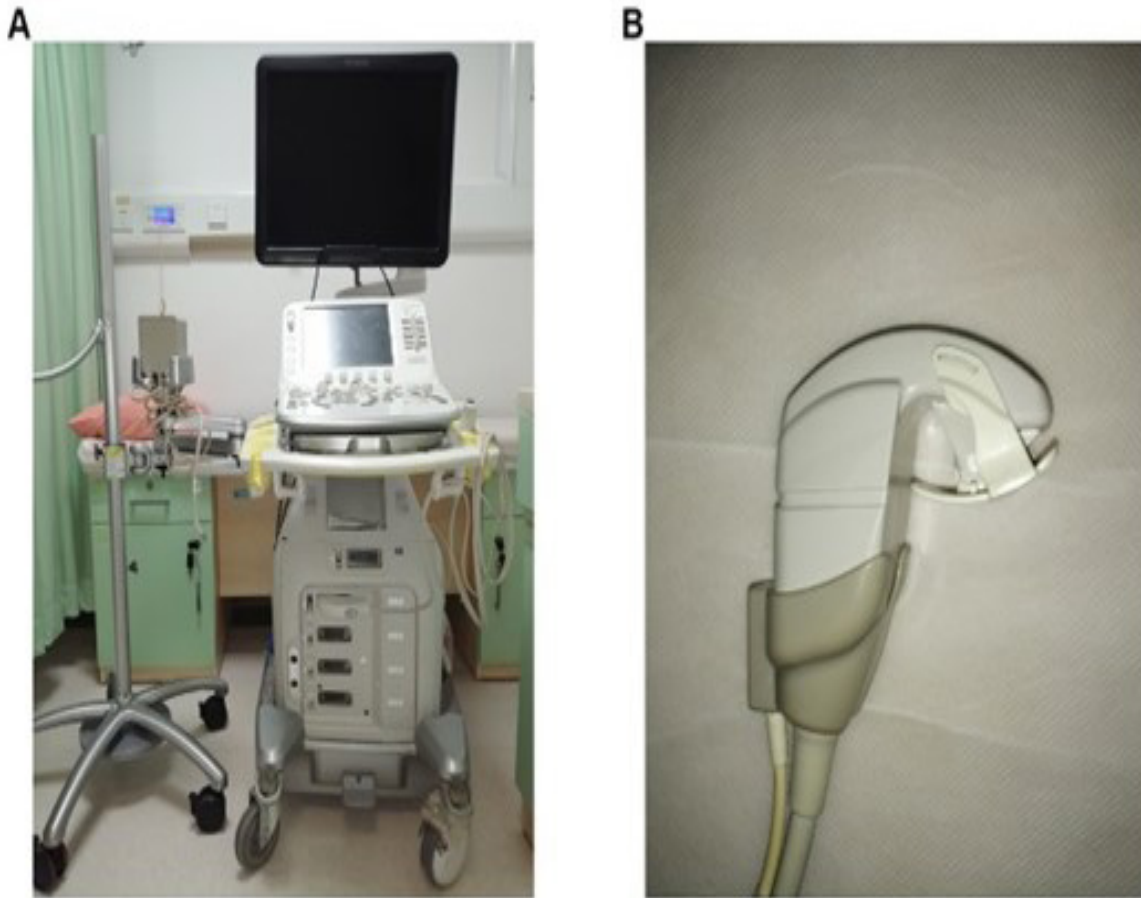


**Figure 2.** The overview of the ARIETTA 70 ultrasound system. (A) ARIETTA 70 ultrasound system. (B) Probe

the operation, the integrated image was matched with the real-time puncture guidance through the iPad, and the simulated image of the puncture pathway was displayed on the screen. The limitations of this method were the additional CT examination and operation time. The Sonix-GPS system was another technology designed to track needle positioning under ultrasound guidance<sup>(13)</sup>. This technology applied electromagnetic tracking to identify the needle location and display the planned puncture access. A prospective comparative study reported that the Sonix-GPS system can improve the success rate of a single puncture without increasing the risk of complications<sup>(14)</sup>. However, the ultrasound image was greatly affected in obese patients. In addition, the Uro-Dyna-CT system reported by Ritter et al.<sup>(15)</sup> was a modified angiography device that allowed 3D reconstruction of CT images and showed the exact pathway chosen for puncture. This device offered a 3D anatomical image with the characteristics of safe, fast, and accurate. The disadvantages included high radiation exposure, high costs, and difficulty in learning. In the research, we demonstrated an innovative technique for kidney puncture. The RVS technology combined the images of ultrasound and CT, allowing the surgeon to puncture with both ultrasound and CT images simultaneously. CT images can provide the information including the diameter and location of kidney stones, the anatomy of the renal pelvis and calyces, and the refined construction of surrounding organs. During

the puncture process, the surgeon can refer to the ultrasound and CT images at the same time, thereby increasing the accuracy of the percutaneous kidney access. The image fusion technology can improve the effectiveness of stone removal of the percutaneous access and reduce the damage to adjacent organs without increasing the risk of radiation exposure and complications. The image fusion technology can be of great help to beginners because of the high success rate of the CT-ultrasound group, which was operated by a urological intern in the whole study. In addition, our results verified the effectiveness of this technology through an *in vitro* pig kidney model and simulated CT-ultrasound fusion study. However, there are some limitations in our research. First, our study lacked a description of the intraoperative application of this technique. At present, our center has tested this technique during surgery, whose results will be published in another manuscript. Second, after the fusion is completed, slight movements of the patient's body, such as breathing activity, can easily reduce the accuracy of the fusion image. During the puncture process, the anesthesiologist can decrease the patient's tidal volume to reduce the impact of breathing activity on the fusion image. Finally, the fusion image cannot be used for the second puncture, as the first puncture changes the structure of the kidney and stones.

## CONCLUSIONS

Our research demonstrated an innovative CT-ultra-

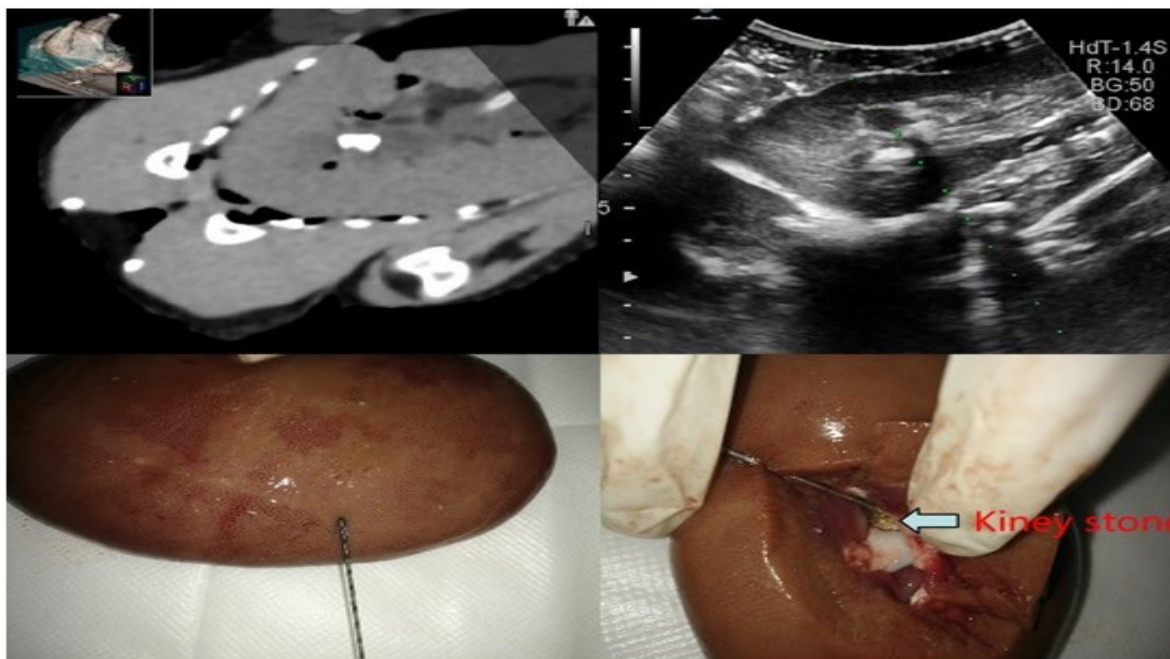


**Figure 3.** The CT-ultrasound fusion images and puncture outcomes with the in vitro pig kidney model

sound image fusion technique for percutaneous kidney puncture. The in vitro study revealed that compared with the traditional ultrasound guidance, the CT-ultrasound fusion imaging technique can shorten the ultrasound screening time, and improve the success rate of puncture. The simulated CT-ultrasound fusion research suggested that this technology can shorten the learning curve and ultrasound screening time. In summary, the

image fusion assisted percutaneous kidney puncture appeared to be safe and effective for PCNL.

**CONFLICT OF INTEREST**

The authors declare that they have no competing interests. This work was funded by grants from the National Natural Science Foundation of China (Grant numbers: 81572511, 81702525, 81702528), Guangzhou Science

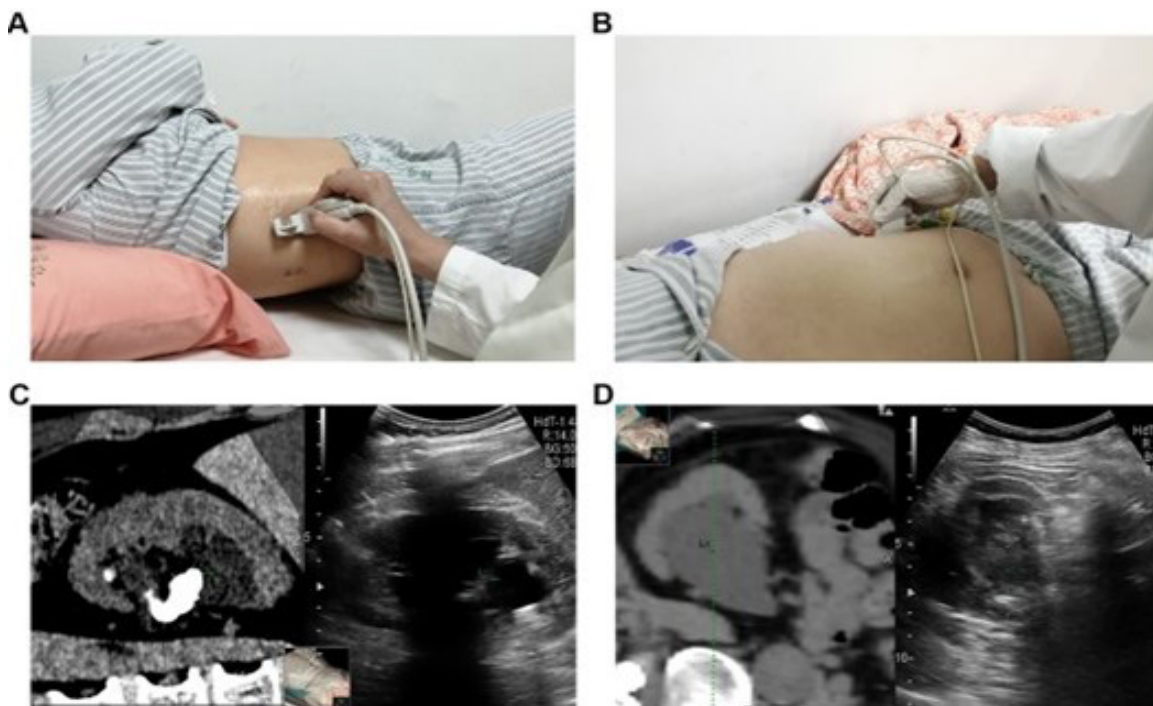


**Figure 4.** Simulated CT-ultrasound image fusion. (A) Simulated CT-ultrasound fusion on the right kidney; (B) Simulated CT-ultrasound fusion on the left kidney; (C) CT-ultrasound fusion image on the right kidney; (D) CT-ultrasound fusion image on the left kidney

and Technology Program key projects (Grant numbers: 201803010029), Natural Science Foundation of Guangdong Province (Grant numbers: 2016A030313317), Medical Scientific Research Foundation of Guangdong Province (Grant numbers: C2018060), and Yixian Clinical Research Project of Sun Yat-sen Memorial Hospital (Grant numbers: sys-c-201802).

15. Ritter M, Rassweiler MC, Michel MS. The Uro Dyna-CT Enables Three-dimensional Planned Laser-guided Complex Punctures. *Eur Urol.* 2015;68:880-4.

## REFERENCES

1. Turk C, Petrik A, Sarica K, et al. EAU Guidelines on Interventional Treatment for Urolithiasis. *Eur Urol.* 2016;69:475-82.
2. Michel MS, Trojan L, Rassweiler JJ. Complications in percutaneous nephrolithotomy. *Eur Urol.* 2007;51:899-906; discussion
3. Patel RM, Okhunov Z, Clayman RV, Landman J. Prone Versus Supine Percutaneous Nephrolithotomy: What Is Your Position? *Curr Urol Rep.* 2017;18:26.
4. de la Rosette JJ, Laguna MP, Rassweiler JJ, Conort P. Training in percutaneous nephrolithotomy--a critical review. *Eur Urol.* 2008;54:994-1001.
5. Rodrigues PL, Rodrigues NF, Fonseca J, Lima E, Vilaça JL. Kidney targeting and puncturing during percutaneous nephrolithotomy: recent advances and future perspectives. *J Endourol.* 2013;27:826-34.
6. de la Rosette J, Kashi AH, Farshid S. Newer Advances in Access. In: Agrawal MS, Mishra DK, Somani B, eds. *Minimally Invasive Percutaneous Nephrolithotomy.* Singapore: Springer Singapore; 2022:145-55.
7. Brisbane W, Bailey MR, Sorensen MD. An overview of kidney stone imaging techniques. *Nat Rev Urol.* 2016;13:654-62.
8. Xu ZF, Xie XY, Kuang M, et al. Percutaneous radiofrequency ablation of malignant liver tumors with ultrasound and CT fusion imaging guidance. *J Clin Ultrasound.* 2014;42:321-30.
9. Hacker A, Wendt-Nordahl G, Honeck P, Michel MS, Alken P, Knoll T. A biological model to teach percutaneous nephrolithotomy technique with ultrasound- and fluoroscopy-guided access. *J Endourol.* 2007;21:545-50.
10. Fernstrom I, Johansson B. Percutaneous pyelolithotomy. A new extraction technique. *Scand J Urol Nephrol.* 1976;10:257-9.
11. Hajiha M, Baldwin DD. New Technologies to Aid in Percutaneous Access. *Urol Clin North Am.* 2019;46:225-43.
12. Rassweiler JJ, Müller M, Fangerau M, et al. iPad-assisted percutaneous access to the kidney using marker-based navigation: initial clinical experience. *Eur Urol.* 2012;61:628-31.
13. Li R, Li T, Qian X, Qi J, Wu D, Liu J. Real-time ultrasonography-guided percutaneous nephrolithotomy using SonixGPS navigation: clinical experience and practice in a single center in China. *J Endourol.* 2015;29:158-61.
14. Li X, Long Q, Chen X, He D, He H. Real-time ultrasound-guided PCNL using a novel SonixGPS needle tracking system. *Urolithiasis.* 2014;42:341-6.